A Series of Related Nucleotide Analogues that Aids Optimization of Fluorescence Signals in Probing the Mechanism of P-Loop ATPases, Such as Actomyosin†

Martin R. Webb,* Gordon P. Reid, V. Ranjit N. Munasinghe, and John E. T. Corrie

National Institute for Medical Research, Mill Hill, London NW7 1AA, United Kingdom

Received June 30, 2004; Revised Manuscript Received September 2, 2004

ABSTRACT: We have synthesized a set of ATP and ADP analogues that have a fluorophore linked to the nucleotide via the 3′-position of the ribose moiety. Combinations of three different coumarins are each attached via different length linkers. A linker based on propylenediamine increases the separation between the nucleotide and fluorophore relative to that of the previously reported ethylenediamine-linked coumarin nucleotides [Webb, M. R., and Corrie, J. E. T. (2001) *Biophys. J. 81*, 1562−1569]. A synthesis of 3′-amino-3′-deoxyATP is described using a combination of chemical and enzymatic procedures, mostly from published methods for synthesis of this compound but with some modifications that improved the convenience of the experimental procedures. This compound is used as a basis of a series of analogues with effectively a zero-length linker. Fluorescence properties of all these analogues are described, together with the kinetics of their interaction with rabbit skeletal myosin subfragment 1 in the presence and absence of actin. One particular analogue, deac-aminoATP [3′-(7-diethylaminocoumarin-3-carbonylamino)-3′-deoxyadenosine 5′-triphosphate], shows a 17-fold enhancement of fluorescence upon binding to this (skeletal) myosin II. As the diphosphate, it exhibits a large signal change upon dissociation from the actomyosin, with kinetics similar to those of natural ADP. The ability of this set of analogues to produce large signals indicated potential uses when scarce proteins are studied in small amounts.

Actomyosin ATPase drives muscle contraction and a variety of cell motility functions through a series of protein conformation changes. The transitions between different nucleotide states during the ATP hydrolysis cycle both change the structure of the protein complex and modulate the degree of interaction between actin and myosin. This hydrolysis in turn enables the cyclical interaction of actin and myosin that in muscle causes the filaments to slide relative to each other. The same general mechanism applies to the wide range of non-muscle myosins, although the dynamics of the reaction may be quite different: different myosins have different kinetics for particular biochemical steps, causing, for example, changes in the "duty ratio". This ratio is the proportion of time in each cycle that the two proteins remain complexed. A low proportion may be suitable when the proteins are filamentous and rapid movement is needed. Attachment for a high proportion of the time is generally required to stop nonfilamentous myosins from diffusing away from the actin during the ATPase cycle.

In a wider sense, the ATP or GTP hydrolysis cycle of a large range of proteins modulates structural changes and protein−protein interactions that are essential for the related biological function. An example is the family of small G proteins that are widely involved in cell signaling and behave as molecular switches. They have an active state when GTP is bound and are inactive when the nucleotide is hydrolyzed to GDP.

To understand this relationship among nucleoside triphosphate hydrolysis, structural changes, and biological function such as mechanochemical coupling in muscle, various probes for examining particular parts of the ATPase cycle have been developed. Because of its sensitivity and time resolution, fluorescence is an important tool in this respect. It can report both binding events and structural changes, although a range of measurements may be required for definitive identification of the process responsible for the signal change. Thus, fluorescence methods are valuable in probing the ATPase cycle on a range of organizational levels from muscle fibers to isolated proteins in solution and to single molecules.

Intrinsic tryptophans have been widely used to provide fluorescence reporter signals in proteins, although it is not always possible to isolate or identify particular processes in this way. The design of specific tryptophan mutants of myosin has enhanced this method (*1*, *2*). This powerful approach provides information that can be localized to particular regions of the protein, and it is particularly suited to isolated proteins that can be engineered in this way. Fluorescent nucleotide analogues provide an alternative, complementary route to obtaining information about changes during the ATPase cycle, and a wide variety of such compounds has been synthesized (*3*, *4*). In particular, labeling at the ribose hydroxyl groups has been useful because this modification does not usually have a large effect on the biochemical properties with P-loop ATPases and GTPases. In principle, almost any organic fluorophore could be attached here. In the case of myosin and various other nucleoside triphosphatases, the 2′- and/or 3′-hydroxyls of the

† This work was supported by the Medical Research Council, U.K., and in part by NIH Grant HL 19242-27.

* To whom correspondence should be addressed. Telephone: (+44) 20 8816 2078. Fax: (+44) 20 8906 4477. E-mail: mwebb@nimr.mrc.ac.uk.

10.1021/bi0486334 CCC: $27.50
Published on Web 10/21/2004

bound nucleotide project from the catalytic site into the medium, so the fluorophore lies on or near the surface of the protein (*5*). In this position, it may respond to both binding and dissociation of the nucleotide, and potentially also to conformation changes in this region of the protein.

In practice, several laboratories have shown that the interaction of fluorescent nucleotides with P-loop ATPases and GTPases differs depending on whether the modification is at the 2′- or 3′-position of the ribose. This may result in different fluorescence properties, kinetics, or affinity. In some cases, there is a clear preference for binding of one isomer. MantADP[1] binds to *Dictyostelium discoideum* myosin II preferentially as the 3′-isomer (*6*). The small G protein Rac preferentially binds the 3′-isomers of coumarin-edaGDPs (*7*). In other cases, both isomers bind but give different fluorescence signals (*8*−*11*), including the case in which fluorescent eda-nucleotides bind to skeletal S1 (*12*). This information together with structural considerations suggests that for many myosins and small G proteins the 3′-isomers may bind with less obstruction by surface amino acids.

Previously, we have synthesized a series of coumarin-labeled nucleotides, coupled to the nucleotide via an ethylenediamine linker (edaADP, etc.; see Figure 1c) (*8*). These analogues provided a signal for monitoring ADP release from skeletal actomyosin. In other examples of interaction of the fluorophore with the surface of a protein, even small changes in the linker or fluorophore can have profound changes on signal response (*13*, *14*). It has also been shown that the eda-based analogues have large differences in fluorescence response (amplitude and direction of signal), depending on the particular myosin (*8*, *15*, *16*) or other proteins to which they are bound. An unusual example of this was found in work on the interaction of several coumarin−eda-guanosine nucleotide conjugates with the small G proteins Rac and Ras. The 3′-mbc-edaGDP analogue, when bound to these proteins, had a large fluorescence response to the presence of bound Mg^{2+} and to P_i, as well as to nucleotide binding (*7*). Other coumarin-labeled analogues only showed small fluorescence changes on nucleotide binding and were unresponsive to the presence of bound Mg^{2+} or P_i. These results show that changes in fluorescence in either direction (increase or decrease) from that of the fluorophore in free solution may provide useful signals.

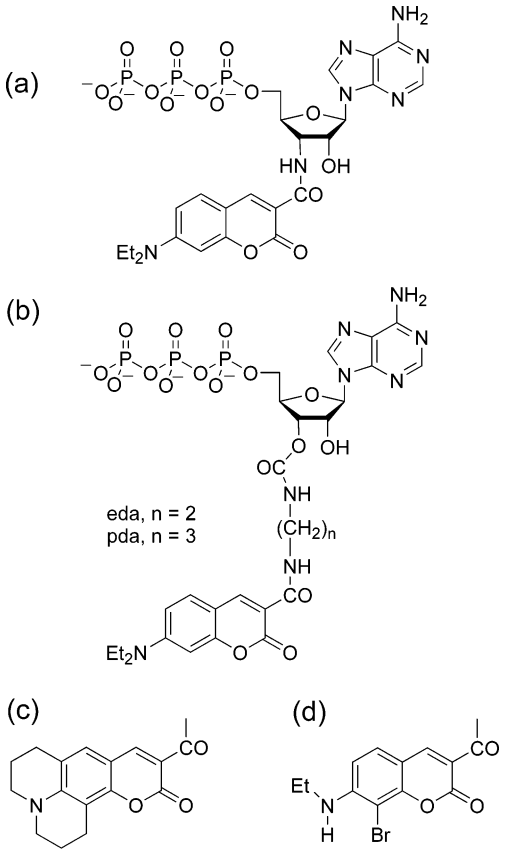

FIGURE 1: Structures of adenosine nucleotide analogues with different linkers. The structures show the 7-diethylaminocoumarin (deac) derivatives: (a) deac-aminoATP and (b) deac-edaATP and deac-pdaATP. Panels c and d show the coumarin 343 (butterfly coumain) and mbc residues, respectively, that replace the deac residue for the other coumarin conjugates.

To use the full potential of fluorophore-labeled nucleotides, it is evidently advantageous to test a range of fluorophores and linkers when optimizing the signal for a particular type of measurement. This work describes the preparation, characterization, and use of a series of nucleotide analogues with free amines attached to the 3′-position of the ribose. In this way, a variety of labels can be linked to the amine at controllable, but different, distances from the ribose or with different structural relationships to it. This should result in a range of analogues in which any one label could have a variety of spatial interactions with the protein surface when the analogues are bound to the protein. The varying spatial relationships may result in different fluorescence properties.

We describe here novel coumarin-labeled nucleotides with longer and shorter linkers, to complement those based on edaATP (Figure 1). One type has a propylenediamine linker (pda) and so places the fluorophore one bond farther from the ribose than the ethylenediamine linker of edaATP. The other type has the fluorescent label coupled directly to the amine group on the ribose ring of 3′-amino-3′-deoxyATP, so it could be considered to have a zero-length linker. Figure 1 shows the structures of the different coumarin conjugates of the amine-modified nucleotides.

To implement this work, we required 3′-amino-3′-deoxyATP. A range of synthetic routes to this nucleotide, based on modification of natural nucleosides, purination of a modified ribose derivative, or isolation from natural sources, have been described: a detailed review is beyond

[1] Abbreviations: mantADP, 2′(3′)-*O*-(*N*-methylanthraniloyl)ADP; S1, myosin subfragment 1; edaATP, 2′(3′)-*O*-[*N*-(2-aminoethyl)-carbamoyl]ATP; pdaATP, 2′(3′)-*O*-[*N*-(3-aminopropyl)carbamoyl]ATP; coumarin 343, 2,3,6,7-tetrahydro-11-oxo-1*H*,5*H*,11*H*-[1]benzopyrano-[6,7,8-*ij*]quinolizine-10-carboxylic acid; coumarin 314, ethyl 2,3,6,7-tetrahydro-11-oxo-1*H*,5*H*,11*H*-[1]benzopyrano[6,7,8-*ij*]quinolizine-10-carboxylate; deac-aminoATP, 3′-(7-diethylaminocoumarin-3-carbonyl-amino)-3′-deoxyadenosine 5′-triphosphate; but-aminoATP, 3′-(coumarin 343-3-ylamino)-3′-deoxyadenosine 5′-triphosphate (coumarin 343 has been termed a butterfly coumarin); mbc-aminoATP, 3′-(7-ethylamino-8-bromocoumarin-3-carbonylamino)-3′-deoxyadenosine 5′-triphosphate; deac-edaATP, 2′(3′)-*O*-{*N*-[2-(7-diethylaminocoumarin-3-carboxamido)-ethyl]carbamoyl}ATP; but-edaATP, coumarin 343-edaATP; mbc-edaATP, 2′(3′)-*O*-{*N*-[2-(7-ethylamino-8-bromocoumarin-3-carboxamido)-ethyl]carbamoyl}ATP; deac-pdaATP, 2′(3′)-*O*-{*N*-[3-(7-diethylaminocoumarin-3-carboxamido)propyl]carbamoyl}ATP; but-pdaATP, coumarin 343-pdaATP; mbc-pdaATP, 2′(3′)-*O*-{*N*-[3-(7-ethylamino-8-bromocoumarin-3-carboxamido)propyl]carbamoyl}ATP; MDCC, *N*-[2-(1-maleimidyl)ethyl]-7-diethylaminocoumarin-3-carboxamide; MDCC-PBP, A197C mutant of phosphate binding protein of *Escherichia coli* labeled with MDCC; DMF, *N*,*N*-dimethylformamide; TEAB, triethylammonium bicarbonate.

the scope of this work. Our route to the precursor 3′-azido-3′-deoxynucleoside draws on previous work (see below) but with some optimization to improve the practicality of the synthesis. Subsequent conversion to the triphosphate uses a mixed chemoenzymatic approach with final reduction of the azide to the required amino group, facilitating a procedure that is more readily carried out without access to specialized chemical facilities. A few examples of fluorescent nucleotide analogues based on 2′-amino-2′-deoxynucleotides have been described and reviewed (*4*), but to the best of our knowledge, this work is the first for the 3′-isomer.

EXPERIMENTAL PROCEDURES

Proteins. Skeletal myosin subfragment 1 (S1) was prepared by chymotryptic digestion of rabbit skeletal myosin (*17*) and stored in liquid nitrogen at ~1 mM. Concentrations were calculated on the basis of a molecular weight of 115 000 and an $E^{1\%}$(280 nm) of 7.9 cm^{-1}. F-Actin from rabbit skeletal muscle was prepared essentially as described previously (*18*). Concentrations were measured from the absorbance spectra, assuming $E^{1\%}$(290 nm) − $E^{1\%}$(310 nm) = 6.2 cm^{-1}. Creatine kinase was prepared from chicken muscle, and the activity was measured in units as described previously (*19*). Adenylate kinase (from chicken muscle) and hexokinase (from baker's yeast) were lyophilized powders (Sigma) and were stored as concentrated aqueous solutions (500−2000 units/mL) at −80 °C.

Synthesis of 3′-Amino-3′-deoxyATP:*3-Azido-3-deoxy-1,2-di-O-acetyl-5-O-(4-methylbenzoyl)-D-ribofuranose **3***. Sodium azide (17.6 g, 270 mmol) was added to a solution of the triflate **1** [27 g, 61.4 mmol; synthesized as described previously (*20*)] in dry DMF (700 mL), and the mixture was stirred overnight at room temperature. The solvent was evaporated *in vacuo*, and the residue was partitioned between water and diethyl ether. The organic phase was washed with water and brine, dried (Na_2SO_4), and evaporated to a yellow oil (18 g). The ^{1}H NMR spectrum showed azide **2** and the 3,4-dehydrosugar byproduct (signals at 5.85 and 6.12 ppm, respectively) in a 41:59 ratio. Calculations based on the total mass, the respective molecular weights, and the product ratio showed the mixture contained azide **2** (8.0 g, 24 mmol) and the byproduct (10.0 g, 34.5 mmol) in yields of 39 and 56%, respectively.

This mixture (9.5 g) was dissolved in formic acid and water (3:1, v/v; 236 mL) and heated at 50 °C for 1 h. The solution was evaporated *in vacuo*, and the residue was re-evaporated from butanol (2 × 100 mL) and then from toluene (2 × 100 mL) to give a yellow solid that was dried *in vacuo* for 2 h. The solid was dissolved in dry pyridine (144 mL), and acetic anhydride (96 mL, 1 mol) was added in two equal portions. The mixture was stirred for 2 h at room temperature, then poured onto crushed ice (500 g), stirred for 0.5 h, and extracted with chloroform (3 × 150 mL). The organic phase was washed with 1 M hydrochloric acid, saturated aqueous $NaHCO_3$, and brine, dried (Na_2SO_4), and evaporated. Flash column chromatography [silica gel; ethyl acetate/hexanes (1:4)] gave **3** (3.51 g, 9.3 mmol) as a mixture of anomers: ^{1}H NMR (500 MHz, $CDCl_3$) δ 6.17 (0.82H, s, H-1$_\beta$), 6.46 (0.18H, d, J = 4.6 Hz, H-1$_\alpha$).

*3′-Azido-3′-deoxyadenosine **4***. A mixture of hexamethyldisilazane (243 mL, 1.16 mol), trimethylsilyl chloride (25.6 mL, 201.7 mmol), and N^6-benzoyladenine (3.67 g, 15.4 mmol) was heated at 130 °C for 4.5 h under nitrogen (*21*). The solution was cooled and evaporated, re-evaporated from dry toluene (3 × 33 mL), and kept *in vacuo* for 0.5 h. The anomeric mixture of diacetates **3** (4.82 g, 12.8 mmol) was dissolved in dry toluene (64 mL) and added at room temperature to a solution of the crude bis-silylated adenine derivative in dry toluene (64 mL). The slightly turbid solution was warmed to 85 °C under nitrogen for a few minutes, and trimethylsilyl triflate (2.8 mL, 15.4 mmol) was added in one portion. The clear solution was kept at 85 °C for 1 h, cooled, and diluted with ethyl acetate. The solution was washed with saturated sodium hydrogen carbonate and brine, dried (Na_2SO_4), and evaporated. Flash chromatography [silica gel; acetone/diethyl ether (1:4)] gave the N^6-benzoyl-2′-*O*-acetyl-5′-*O*-(4-methylbenzoyl) nucleoside as a pale beige foam (4.36 g, 7.84 mmol, 61%): ^{1}H NMR (500 MHz, $CDCl_3$) δ 2.21 (3H, s, OAc), 2.40 (3H, s, Ar-Me), 4.39−4.42 (1H, m, H-4′), 4.55 (1H, dd, J = 12.5, 4.1 Hz, H-5$_a$), 4.76 (1H, dd, J = 12.5, 3.3 Hz, H-5$_b$), 4.96 (1H, dd, J = 6.9, 6.0 Hz, H-3′), 6.11 (1H, d, J = 3.7 Hz, H-1′), 6.15 (1H, dd, J = 5.8, 3.8 Hz, H-2′), 7.22 (2H, d, J = 7.9 Hz, ArH), 7.52 (2H, t, J = 7.1 Hz, ArH), 7.61 (1H, t, J = 7.4 Hz, ArH), 7.88 (2H, d, J = 8.2 Hz, ArH), 8.01 (2H, d, J = 8.2 Hz, ArH), 8.06 (1H, s, H-2), 8.66 (1H, s, H-8), 8.97 (1H, br s, NH).

The protected nucleoside, the N^6-benzoyl-2′-*O*-acetyl-5′-*O*-(4-methylbenzoyl) derivative of **4** (2.17 g, 3.92 mmol), was dissolved in ammonia-saturated methanol (294 mL), kept at room temperature for 4 days, and then evaporated. The residual solid was dissolved in ethanol and water (1:4, 390 mL) at 60 °C. The solution was cooled to room temperature, and dry Dowex 50 resin (H^+ form, 19.6 mL) was added. The mixture was stirred for 5 min; the solvent was decanted, and the resin was washed with ethanol and water (3:7, 3 × 390 mL), then mixed with 35% aqueous ammonia, ethanol, and water (7:25:18, v/v; 260 mL), and stirred for 2 h at room temperature. The solvent was filtered and retained, and the resin was treated with the same volume of ammonia, ethanol, and water and stirred overnight. The solution was filtered, and the resin was washed with 2 × 20 mL of the same ammonia mixture. The combined filtrates were analyzed by reverse phase HPLC [Merck Lichrospher RP8 250 mm × 4 mm column; mobile phase of acetonitrile and water (1:9, v/v), with a flow rate of 1.5 mL/min]. Nucleoside **4** had a t_R of 13.1 min, and no other peaks were observed. UV analysis (ϵ_{259} = 15 300 M^{-1} cm^{-1}) showed a yield of 3.61 mmol (92%) The solution was evaporated and re-evaporated from methanol to remove all ammonia, and the residue was crystallized from water to give **4** as beige crystals (0.9 g): mp 212−214 °C [lit. (*22*) mp 218−220 °C]; ^{1}H NMR (500 MHz, DMSO-d_6 and D_2O) δ 3.61 (1H, dd, J = 12.4, 3.4 Hz, H-5$_a$), 3.70 (1H, dd, J = 12.4, 3.4 Hz, H-5$_b$), 4.02 (1H, m, H-4′), 4.32 (1H, dd, J = 5.4, 3.6 Hz, H-3′), 5.00 (1H, t, J = 5.9 Hz, H-2′), 5.91 (1H, d, J = 6.2 Hz, H-1′), 8.18 (1H, s, H-2), 8.37 (1H, s, H-8).

*3′-Azido-3′-deoxyAMP **5***. Phosphorus oxychloride (233 μL, 2.5 mmol) was added to a suspension of 3′-azido-3′-deoxyadenosine **4** (292 mg, 1.0 mmol) in triethyl phosphate (4.25 mL), and the mixture was stirred at 0 °C for 1.5 h, then diluted with water (200 mL), and adjusted to pH 7.4. Anion-exchange chromatography [2.5 cm × 40 cm DEAE-cellulose column, eluted with a linear gradient formed from

10 and 250 mM TEAB (each 1000 mL)] gave one main UV-absorbing peak, which was analyzed by anion-exchange HPLC [Whatman Partisphere SAX 4.6 mm × 125 mm column; mobile phase of 25 mM NaH_2PO_4, adjusted to pH 6 with NaOH, containing methanol (100:13, v/v), with a flow rate of 1.5 mL/min] and showed a single peak at $t_R = 3.3$ min, corresponding to monophosphate **5**. UV spectrophotometry ($\epsilon_{260} = 15\,300\ M^{-1}\ cm^{-1}$) gave the yield as 855 μmol. The solution was evaporated *in vacuo*, and then re-evaporated from methanol (three times). The residue was dissolved in water (10 mL) and frozen. A portion (25 μmol) was converted to the sodium salt (Dowex 50, Na form): ^{1}H NMR (500 MHz, D_2O) δ 4.00−4.01 (2H, br m, H-5′), 4.38 (1H, br s, H-4′), 4.55 (1H, dd, $J = 5.4$, 3.4 Hz, H-3′), 5.09 (1H, t, $J = 6.0$ Hz, H-2′), 6.11 (1H, d, $J = 6.4$ Hz, H-1′), 8.26 (1H, s, H-2), 8.62 (1H, s, H-8).

*3′-Amino-3′-deoxyATP **7***. A solution of monophosphate **5** (500 μmol) in 100 mL of 100 mM Tris-HCl buffer (pH 7.5) was incubated for ∼2 h at room temperature after the following components were added (final concentrations): 5 mM $MgCl_2$, 100 μM ATP, 20 mM creatine phosphate, 5 units/mL adenylate kinase, and 5 units/mL creatine kinase. The reaction was followed by anion-exchange HPLC [SAX column as described above, mobile phase of 0.4 M $(NH_4)_2HPO_4$, adjusted to pH 4.0 with concentrated HCl, with a flow rate of 1.5 mL/min]. Elution times were 4.9 min for 3′-azido-3′-deoxyATP, 2.4 min for 3′-azido-3′-deoxyADP, and 1.6 min for 3′-azido-3′-deoxyAMP. Conversion to 3′-azido-3′-deoxyATP **6** was ∼95% based on HPLC. The incubate was adjusted to pH 7.4 with 1 M HCl and diluted to 800 mL. Anion-exchange chromatography (column as in purification of **5** described above) with a linear gradient formed from 10 and 450 mM TEAB (each 1000 mL) gave one main peak, eluting at ∼230 mM TEAB. Analysis of fractions by anion-exchange HPLC [SAX column as described above, mobile phase of 0.3 M sodium phosphate (pH 6) and methanol (100:13, v/v), with a flow rate of 1.5 mL/min] showed a principal component with a t_R of 4.5 min, assigned as azido triphosphate **6**. Fractions toward the end of the eluted material showed traces of a poorly resolved peak attributed to ATP ($t_R = 5.2$ min), but no attempt was made to separate this from the main fraction. The combined fractions, quantified by UV spectrophotometry, contained 454 μmol of nucleoside triphosphates (i.e., **6** with ATP). This mixture was evaporated *in vacuo* and re-evaporated from methanol (three times), and the residue was dissolved in water (5.4 mL) and 35% aqueous ammonia (w/v, 16.2 mL) and treated with a solution of triphenylphosphine (1.17 g) in pyridine (32.4 mL). The flask was flushed with nitrogen and then sealed, and the contents were stirred overnight at room temperature. The solution was diluted with water (180 mL) and extracted with diethyl ether (3 × 180 mL). The aqueous solution was evaporated *in vacuo* and re-evaporated twice from water. The residue was dissolved in water (800 mL) and adjusted to pH 7.4. Anion-exchange chromatography (column as in purification of **5** described above) with a linear gradient formed from 10 and 400 mM TEAB (each 1000 mL) gave one peak that eluted at ∼250 mM TEAB. Fractions across this peak, analyzed by anion-exchange HPLC (SAX column and mobile phase as described for **6**), showed its principal component **7** at 3.6 min (t_R), with essentially no cross contamination by ATP. UV spectrophotometry showed a yield of 346 μmol. A trace of 3′-aminoADP ($t_R = 1.6$ min) was present in the earliest fractions of the main peak. These early fractions were not combined with fractions containing pure **7**. The latter were evaporated *in vacuo* and re-evaporated from methanol (three times), and the residue was dissolved in water (10 mL) and frozen. A portion (5 μmol) was converted to the sodium salt (Dowex 50, Na form): ^{1}H NMR (500 MHz, D_2O) δ 4.11 (1H, dt, $J = 11.7$, 3.2 Hz, H-5$_a$), 4.16 (1H, t, $J = 6.7$ Hz, H-3′), 4.28 (1H, ddd, $J = 11.9$, 7.1, 2.4 Hz, H-5$_b$), 4.41−4.43 (1H, m, H-4′), 4.72 (1H, dd, $J = 6.1$, 3.2 Hz, H-2′), 5.98 (1H, d, $J = 3.2$ Hz, H-1′), 8.01 (1H, s, H-2), 8.23 (1H, s, H-8); ^{31}P NMR [D_2O with 2 mM EDTA and 20 mM MOPS (pH 7.0)] δ −9.72 (d, $J = 20.8$ Hz, P_γ), −14.15 (dt, $J = 19.5$, 4.7 Hz, P_α), −24.81 (t, $J = 20.1$ Hz, P_β); LRMS (negative ion ES) found *m*/*z* 505, calcd for $C_{10}H_{16}N_6O_{12}P_3^-$ 505.

3′-Amino-3′-deoxyADP. The hexokinase-catalyzed phosphorylation of glucose provided a convenient method of preparing the diphosphate. The following were incubated at room temperature in 50 mM Tris-HCl (pH 7.5), 10 mM KCl, 5.1 mM $MgCl_2$, 5 mM 3′-amino-3′-deoxyATP, 10 units/mL hexokinase, and 10 mM glucose. The reaction was followed by HPLC as described above and was essentially complete (>95%) in ∼4.5 h. The product (on a 50 μmol scale) was purified on a column of DEAE-cellulose (1.6 cm × 30 cm) with a linear gradient from 10 and 500 mM TEAB (each 500 mL). 3′-Amino-3′-deoxyADP was concentrated and stored as described above.

Synthesis of Coumarin-Labeled Nucleotides. The pdaATP and pdaADP analogues were prepared and used to synthesize the mixture of 2′- and 3′-coumarin derivatives, which were then separated by chromatography, using methods similar to those of the eda analogues (*8*, *23*, *24*). 3′-Amino-3′-deoxyATP was coupled to coumarin carboxylic acids by activating the acids as their mixed anhydrides. The method is exemplified for the 7-diethylaminocoumarin-3-carboxylate conjugate.

7-Diethylaminocoumarin-3-carboxylic acid (16.4 mg, 62.8 μmol) was activated by dissolving it in dry DMF (1 mL), cooling it on ice, and adding tributylamine (25 μL, 103 μmol) and isobutyl chloroformate (10 μL, 77 μmol). The reaction mixture was left on ice for 50 min. 3′-Amino-3′-deoxyATP (40 μmol, triethylammonium salt) in water (300 μL) was added to the activated coumarin and stirred at room temperature for 2 h. HPLC analysis was carried out with the reaction mixture [Partisphere SAX as described above, with 0.4 M $(NH_4)_2HPO_4$, adjusted to pH 4.0 with concentrated HCl, with 5% (v/v) acetonitrile; flow rate of 1.5 mL/min]. Elution times were 1.6 min for 7-diethylaminocoumarin-3-carboxylic acid, 3.5 min for 3′-amino-3′-deoxyATP, and 13 min for deac-aminoATP. The reaction mixture was applied to a DEAE-cellulose column (1.6 cm × 30 cm) equilibrated in 10 mM TEAB and eluted with a TEAB gradient from 10 to 600 mM (total volume of 1 L). The product deac-aminoATP was concentrated as described above and stored frozen. Its concentration was determined from its UV−visible spectrum ($\epsilon_{429} = 46\,800\ M^{-1}\ cm^{-1}$), and on this basis, the yield was 80%.

A portion of the conjugate was converted to its Na salt: ^{1}H NMR (500 MHz, D_2O) δ 1.20 (6H, t, $J = 6.9$ Hz, C*H*$_3$-CH$_2$), 3.47 (4H, q, $J = 6.9$ Hz, CH$_3$C*H*$_2$), 4.28−4.31 (1H, m, H-5$_a$), 4.37−4.40 (1H, m, H-5$_b$), 4.57−4.59 (1H, m, H-4′),

4.84 (1H, t, $J = 6.1$ Hz, H-3′), 4.93 (1H, dd, $J = 6.1$, 4.1 Hz, H-2′), 6.21 (1H, d, $J = 4.1$ Hz, H-1′), 6.49 (1H, d, $J = 1.6$ Hz, coumarin H-8), 6.75 (1H, dd, $J = 9.0$, 1.6 Hz, coumarin H-6), 7.44 (1H, d, $J = 9.0$ Hz, coumarin H-5), 8.15 (1H, s, H-2), 8.48 (1H, s, coumarin H-4), 8.53 (1H, s, H-8); ^{31}P NMR (^{1}H-decoupled) δ −13.05 (d, $J = 18.3$ Hz, P_γ), −14.12 (d, $J = 18.9$ Hz, P_α), −25.6 (t, $J = 18.2$ Hz, P_β); LRMS (negative ion MALDI) found *m/e* 748, calcd for $C_{24}H_{29}N_7O_{15}P_3^-$ 748.

The equivalent diphosphate of each analogue was prepared from the parent diphosphate or by myosin subfragment 1-catalyzed hydrolysis of the triphosphate. The other coumarin−aminoATP and −ADP conjugates were prepared similarly.

Steady-State ATPase Activity. The rate of hydrolysis of each ATP analogue by acto-S1 was measured at 20 °C by HPLC analysis of the nucleotides to obtain the extent of hydrolysis at different times (*8*). The buffer was 10 mM PIPES (pH 7.0) and 1 mM $MgCl_2$; this buffer at 20 °C was used for all measurements unless indicated otherwise. The steady-state ATPase activity by S1 alone was measured at 20 °C using the fluorescent phosphate sensor, MDCC-PBP (*13*). ATP or analogue (10 μM) was incubated with 10 μM MDCC-PBP. The fluorescence was followed with time using 430 nm excitation and 465 nm emission. The fluorescence signal was calibrated using P_i at a known concentration.

Other Measurements. Absorbance spectra were obtained on a Beckman DU460 spectrophotometer. Concentrations of the nucleotide were determined from the coumarin absorbance as well as the absorbance of adenosine at 260 nm, after correction for absorbance due to the coumarin at this wavelength. The two measurements generally were within 10% of each other. The coumarin extinction coefficients were those obtained for the parent coumarin carboxylic acids as simple esters or amides. For deac, these values are 46 800 M^{-1} cm^{-1} at 430 nm and 12 800 M^{-1} cm^{-1} at 260 nm (*25*). For mbc, these values are 34 500 M^{-1} cm^{-1} at 410 nm and 10 300 M^{-1} cm^{-1} at 260 nm (*26*). For the butterfly coumarin, the values are 45 000 M^{-1} cm^{-1} at 436 nm and 7660 M^{-1} cm^{-1} at 260 nm (*27*). The maximum wavelength of coumarin absorbance shifts depending on the chemical environment, but the extinction coefficient is not significantly altered (*25*).

Fluorescence measurements were obtained on a Perkin-Elmer LS50B fluorimeter with a xenon lamp. Stopped-flow experiments were carried out in a HiTech SF-61 DX2 apparatus, with a mercury−xenon lamp and HiTech Kinet Asyst software. There was a monochromator and 5 nm slits on the excitation light (436 nm) and a 455 nm cutoff filter on the emission. All measurements were taken in 10 mM PIPES (pH 7.0) and 1 mM $MgCl_2$ at 20 °C, unless otherwise stated. Data were fitted using the HiTech software or Grafit (*28*).

RESULTS

Synthesis of 3′-Amino-3′-deoxyATP. This was based on known methods with some modifications that improved the convenience of experimental procedures. The synthetic route is outlined in Figure 2. Triflate **1** (*20*) was reacted with sodium azide in DMF (*29*) to give azide **2**, accompanied by elimination to give the 3,4-dehydrosugar derivative in a similar proportion. Although this mixture could be separated,

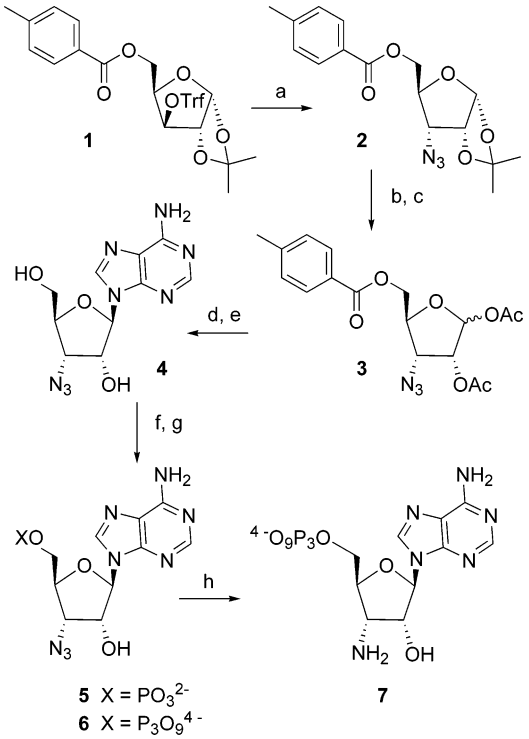

FIGURE 2: Reaction scheme for synthesis of 3′-amino-3′-deoxyATP: (a) NaN_3·DMF, (b) HCO_2H·water, (c) Ac_2O·pyridine, (d) silylated N^6-benzoyladenine·TMS triflate·toluene, (e) aqueous ammonia-MeOH, then Dowex 50 (H^+), (f) $POCl_3$·$(ETO_3)PO$, (g) adenylate kinase·creatine phosphate·ATP·creatine kinase, (h) triphenylphosphine·aqueous NH_3·pyridine.

it was feasible to use the crude mixture for acetolysis of the protecting isopropylidene group (*20*) to give the epimeric diacetates **3**. This mixture was satisfactory for use in the purination with the disilylated derivative of N^6-benzoyladenine in the presence of trimethylsilyl triflate (*30*). Subsequent removal of all protecting groups with methanolic ammonia gave 3′-azido-3′-deoxyadenosine **4** as the pure β-anomer. Note that in the α-anomer, the H-1′ signal would be ∼0.35 ppm downfield of that in the β-anomer (*31*): thus, an accurate assessment of anomeric purity is readily available. This material was converted to 5′-monophosphate **5** by the method of Yoshikawa et al. (*32*).

Chemical synthesis of the triphosphate by a method based on that of Hoard and Ott (*33*) gave variable, generally low yields: enzymatic transformation was therefore used to synthesize the azido triphosphate. Monophosphate **5** is a poor substrate for adenylate kinase, with an activity (V_{max}), only a few percent of the rate with AMP itself. However, this rate is sufficient to use this enzyme, together with a very small quantity of ATP, to phosphorylate **5** to the corresponding 5′-diphosphate. The ADP and 3′-azido-3′-deoxyADP concurrently formed in this process are both readily and essentially quantitatively phosphorylated to their triphosphates by creatine kinase and creatine phosphate.

In principle, the crude enzyme incubate, after formation of the triphosphate, could simply be lyophilized and used directly for Staudinger reduction of the azido group (*22*) to yield amino triphosphate **7**. However, in practice, it was preferable to perform anion-exchange chromatography after both the enzymatic and chemical steps. Overall, azido monophosphate **5** was converted to amino triphosphate **7** in 70% yield on a scale of 500 μmol. 3′-Amino-3′-deoxyATP

Table 1: Fluorescence Properties of the Coumarin-Labeled Nucleotides Alone and upon Interaction with Skeletal Myosin Subfragment 1 (S1)

	fluorescence quantum yield[a]		fluorescence ratio[b]	excitation maximum	emission maximum (nm)	
	−S1	+S1	(+S1/−S1)	(nm) (−S1)	−S1	+S1
3′-deac-pdaADP	0.06	0.01	0.24	428	475	472
3′-mbc-pdaADP	0.70	0.08	0.20	408	465	460
3′-but-pdaADP	0.64	0.17	0.26	448	488	492
3′-deac-aminoADP	0.02	0.31	17	432	477	480
3′-mbc-aminoADP	0.76	0.48	0.63	405	461	458
3′-but-aminoADP	0.59	−*c*	−*c*	451	491	−*c*

[a] Values were calculated relative to the fluorescence quantum yield of coumarin 314 in ethanol, 0.83 (*27*). For quantum yield determinations, emission spectra were obtained using solutions with an absorbance of <0.05 cm^{-1} and corrected for the photomultiplier profile and baseline. Measurements in the presence of S1 had 2.1 or 4.2 μM protein added. [b] Ratio of fluorescence intensities at the wavelength of maximum emission. When the ratio is <1, the fluorescence decreases upon binding to S1. [c] The fluorescence change with S1 was very small, so fluorescence measurements were not pursued with this analogue.

was a reasonable substrate for hexokinase, so this enzyme could be used to make 3′-amino-3′-deoxyADP for direct preparation of the coumarin-labeled nucleoside diphosphates.

Synthesis of Coumarin Nucleotides. The synthetic method for pda-linked nucleotides was analogous to that for the eda compounds (*8*, *23*, *34*), and three coumarins (deac, but, and mbc) were attached to the pda linker. As described for the coumarin-labeled eda nucleotides, the three nucleotides with the pda linker resulted in a mixture of 2′- and 3′-isomers in a similar ratio (~40:60) in each case. These isomers interconvert extremely slowly, so could be isolated and stored as single isomers as they separate from each other on ion-exchange chromatography. However, the chromatographic behavior of the pda analogues differed from that of the eda counterparts. All the eda nucleotide isomers (2′ and 3′) show reversal of elution order between two ion-exchange chromatography media, preparative DEAE-cellulose (2′-isomer first) and analytical HPLC Partisphere SAX (3′-isomer first). The pda analogues showed the same order on both types of medium: the 3′-isomer elutes first. Interconversion of the 2′- and 3′-isomers was very slow, as determined for the eda derivatives (*8*). Because of considerations outlined in the introductory section and our previous experience with the eda derivatives, only the 3′-isomers are used in this work to characterize their interaction with S1.

The same three coumarins were attached to the free amine of 3′-amino-3′-deoxyATP, using similar chemistry as with the pda and eda nucleotides. In this case, there is no ambiguity about the position of the attachment of coumarin to the ribose as only the 3′-position contains a group that can react with the fluorescent label.

Fluorescence Properties. Fluorescence properties of each coumarin-labeled ADP or ATP were measured in the presence and absence of skeletal S1 (Table 1). In all cases, the linker had a minimal effect on the fluorescence properties in free solution: the deac derivatives have low fluorescence, while the butterfly and mbc derivatives are much more intensely fluorescent. The pda-linked analogues are qualitatively similar to the eda ones, showing a decrease in fluorescence on binding to S1. However, the analogues derived from 3′-amino-3′-deoxyATP show some large differences. Emission spectra are shown in Figure 3 for deac-aminoADP, which has the largest fluorescence change (17-fold increase in amplitude at the maximum emission wavelength of 480 nm) on binding to skeletal S1. A similarly large increase in fluorescence was shown when deac-aminoATP binds to a myosin I, Myo1b, from rat liver (C. Batters, L. M. Coluccio, J. E. Molloy, and M. R. Webb, unpublished result) or to smooth muscle myosin from chicken gizzard. In contrast, the mbc analogue showed a small decrease in fluorescence on binding to skeletal S1, while but-aminoATP exhibits little or no change in fluorescence, depending on conditions. Because of this, the interaction of but-aminoATP with S1 and acto-S1 was not studied further.

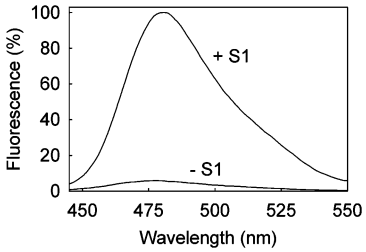

FIGURE 3: Fluorescence change upon binding of deac-aminoADP to S1. Sufficient S1 was added to bind all nucleotide. Deac-aminoADP (0.3 μM) was excited at 435 nm and 10 μM S1 added.

Table 2: Steady-State and Kinetic and Binding Properties of the Coumarin-Labeled Nucleotides with Actomyosin and Myosin Subfragment 1 (S1)[a]

	steady-state ATPase rate[b] (%)		dissociation rate[c] (s^{-1})		K_d (μM)
	S1	AS1	S1	AS1	(S1)[d]
3′-deac-pdaATP/ADP	67	117	1.9	248	1.7
3′-mbc-pdaATP/ADP	88	75	1.1	184	0.8
3′-but-pdaATP/ADP	56	100	1.2	122	0.8
deac-aminoATP/ADP	115	141	3.9	516	0.6
mbc-aminoATP/ADP	61	163	1.1	367	0.8
but-aminoATP/ADP	59	133	−*e*	−*e*	−*e*

[a] Rates were measured in 10 mM PIPES (pH 7.0) and 1 mM $MgCl_2$ at 20 °C. [b] Rates were measured for the triphosphates under one set of conditions and so are given as the percent of the value obtained with ATP. For S1 alone, rates were measured in 10 μM triphosphate and 0.25 μM S1 in the presence of 10 μM MDCC-PBP. The rate of P_i formation was measured by fluorescence. For actoS1 (AS1), the rates were measured with 500 μM triphosphate, 40 μM actin, and 0.2 μM S1. Aliquots were removed at time intervals to measure the diphosphate/triphosphate ratio by HPLC. See the text for details. [c] Kinetics were measured using a stopped-flow apparatus for the diphosphates. For S1 alone, a solution containing 0.25 μM coumarin nucleotide as the diphosphate and 2 μM S1 was mixed rapidly with 50 μM ATP (mixing chamber concentrations). For actoS1, a solution containing 2 μM nucleotide, 10 μM S1, and 40 μM actin was mixed with 4 mM ATP. [d] Dissociation constants were determined for the diphosphates from titrations as in Figure 5, using the appropriate wavelengths as in Table 1. Where there was a shift in the emission maximum upon binding, the wavelength at the highest intensity was used. [e] Not determined.

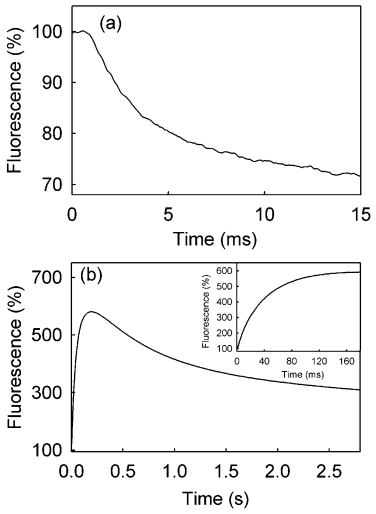

FIGURE 4: Association kinetics of deac-aminoATP and dissociation of deac-aminoADP with actoS1. Kinetics were measured using a stopped-flow apparatus. Concentrations are those in the mixing chamber. Fluorescence was measured as described in the text. (a) A solution containing 2 μM coumarin nucleotide, 10 μM S1, and 20 μM actin was mixed rapidly with 4 mM sodium ATP. (b) Actin (45 μM) with 2.5 μM S1 were mixed with 0.5 μM deac-aminoATP. The inset shows a short time base.

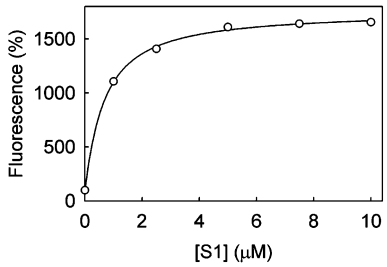

FIGURE 5: Titration of S1 into a solution of deac-aminoADP to obtain the dissociation constant. S1 was added to a solution of 0.1 μM nucleotide, and the fluorescence was monitored at 480 nm, with excitation at 435 nm.

Steady-State ATPase Measurements. To show the extent to which the analogues mimic ATP, the steady-state ATPase rates were measured for one set of conditions. Measurements were taken in the presence of S1 or actoS1, and results are shown in Table 2. All the rates were close to that of ATP. Since this survey of rates was carried out at a single concentration of nucleotide, the variations could be due to relatively minor changes in the values of either k_{cat} or K_m.

Rate Constants for Individual Processes in the Actomyosin ATPase Cycle. To obtain a view of the performance of these analogues with one particular protein, the rates of dissociation from skeletal S1 were determined in the presence and absence of actin. The kinetics were measured using stopped-flow fluorescence, mixing the preformed complex of the nucleotide and S1 (or actoS1) with a large excess of ATP. Data are summarized in Table 2. Figure 4 shows the signal obtained for dissociation of deac-aminoADP from actoS1. This demonstrates that the fluorescence change for this dissociation remains significant, despite some signal being lost due to the instrument dead time and not all nucleotide being bound at time zero due to weak binding. The rate constant is similar to that for ADP (*35*).

Further measurements were carried out using deac-aminoATP and its diphosphate, since these showed the largest fluorescence changes with skeletal S1. In particular, kinetics of binding to S1 alone and to actoS1 were measured (Figure 4). These were similar to values obtained with the eda-linked nucleotides. This measurement also gave an assessment of the fluorescence intensity change upon binding to actoS1. This change is difficult to obtain from steady-state measurements as the lifetime of species bound to actoS1 is very short and the diphosphate binding is weak.

DISCUSSION

The six coumarin-labeled ATP analogues described here, along with the three previously described (*8*), make a set of nine related compounds. This set is comprised of the combinations of three different coumarins with three different linkers, and each compound may differ in both the fluorescence properties *per se* and the interaction of that nucleotide with a protein. The availability of such a series is useful in two ways. First, the best of these analogues for a particular situation can be chosen. Second, the features of the analogues that determine their properties can be compared, potentially leading to rational development of other analogues with improved properties. These two aspects will be discussed, after assessment of the properties of the six analogues described here and their interaction with skeletal S1 and actoS1.

There are several generalizations for the set of 3′-modified nucleotides. On the basis of their steady-state activities, all the compounds are reasonably good analogues of ATP or ADP, as predicted in the introductory section for modification at this position of the ribose moiety. The ATPase rates of the triphosphates with both S1 and actoS1 and the dissociation constants of the diphosphates from S1 are mostly within a factor of 2 of those of the natural nucleotides (Table 2). Thus, there is very little to distinguish the analogues on the basis of such measurements with this myosin.

Examination of single-step kinetics reveals a little more variability between the analogues. While most diphosphate dissociation rate constants are within a factor of 2 of those expected for the natural nucleotides, there are a few exceptions. 3′-Mbc-pdaADP and 3′-but-pdaADP dissociate from actoS1 approximately 3-fold slower than ADP. Deac-aminoADP dissociates approximately 3-fold faster from S1 than ADP. We will return to this later, but even these changes are minor when considered in terms of likely causes due to the interaction of nucleotide with protein. However, it should be noted that the increase in the dissociation rate of deac-aminoADP from S1 is not a direct correlation with the change in dissociation constant, based on titration data.

Fluorescence properties of the analogues complexed to S1 show considerable variability. In general, the fluorescence of the bound fluorophore is lower than in free solution. The one notable exception is deac-aminoADP which exhibits a large enhancement from the low fluorescence quantum yield in solution. The other two coumarin adducts with 3′-amino-3′-deoxyADP exhibit only a small decrease (mbc) or little or no change (but-aminoADP, depending on conditions) upon binding. Thus, with skeletal S1, the deac-aminoATP shows the greatest signal change of all nine analogues. Furthermore, the fluorescence *increases* with binding. This is a potential advantage for measuring dissociation kinetics by stopped flow or in muscle fibers. Because the binding of the

diphosphate is often weak with myosins in the presence of actin, there may be significant free nucleotide. Any of the analogue in free solution will only contribute low intensity to the fluorescence background.

In this case, one of the three coumarins exhibits fluorescence behavior significantly different from that of the other two. Furthermore, as described in the introductory section, one coumarin (mbc) attached via the eda linkage to GTP shows very different responses to the other two coumarins with small G proteins. These two examples illustrate the benefit of testing a range of similar analogues.

What can be said about how such differences arise between coumarins and between different linkages? Both the change in fluorescence on binding and the changes in kinetic and thermodynamic parameters are likely to be due to interaction of the fluorophore itself with the protein. By their nature, fluorophores are likely to have several sites that might interact with the protein surface. Particularly with the flexible eda and pda linkers, there is a range of possible positions for the fluorophore around the binding cleft. The fact that the deac-aminoADP has a different fluorescence change from all the other analogues and also is the only one that has dissociation kinetics significantly different from those of ADP suggests that its binding is in some way unique. The 3′-amino-3′-deoxyADP derivatives all have effectively a zero-length linker, implying that the coumarins must reside very close to the nucleotide-binding pocket. Thus, the coumarins attached to 3′-amino-3′-deoxyATP probably do not have the same freedom of movement as the eda- or pda-linked analogues.

The mechanism that is believed to underlie the increased fluorescence of the diethylaminocoumarin is by the bonds at the nitrogen of the diethylamino moiety being held coplanar with the coumarin in the excited state (*36*), thereby maximizing overlap of the nitrogen lone pair with the aromatic system. This also explains the inherently high fluorescence of the butterfly coumarins in solution, where the extra aliphatic rings prevent twisting around the bond between the nitrogen atom and the coumarin nucleus (*37*). In a different example of a diethylaminocoumarin attached directly to a protein, this mechanism was operative: a crystal structure of the phosphate sensor MDCC-PBP showed the coumarin bound in a surface cleft so that the diethylamino group was held coplanar (*38*). It is feasible that the coumarin of deac-aminoADP interacts with the protein surface in this way, and so gives rise to the large enhancement in fluorescence upon binding. However, it is unlikely that this twist mechanism underlies the fluorescence changes found in this and our earlier work upon binding of the other nucleotide analogues to myosin, since the butterfly coumarin derivatives, which cannot twist around the nitrogen ring bond, also exhibit decreased fluorescence upon binding. Possible mechanisms that would lead to a decrease in fluorescence include ring distortion and/or bond twisting at the coumarin carboxyl. Clearly, a detailed structure of a protein complexed with the nucleotide analogue would greatly aid interpretation of the origins of the signal changes.

In summary, we have developed a set of nine related fluorescent ATP and ADP analogues. The coumarin fluorophores provide a compromise between the wavelength and good environmental sensitivity of their fluorescence. Their excitation and emission wavelengths in the visible region are generally well separated from the absorbance of the most prevalent natural molecules. One aim was to be able to choose at least one member of the set of related analogues that gives a good signal for a particular combination of process and protein. Such a strategy is particularly important, given the current need to study proteins that are available in only small amounts, such as the myosin I mentioned above. In such cases, signal maximization is needed to overcome the dilute solutions or small volumes inherent in studying such scarce proteins.

ACKNOWLEDGMENT

We thank Mrs. J. Hunter (National Institute for Medical Research) for preparing skeletal muscle myosin subfragment 1 and F-actin, the EPSRC Mass Spectrometry Centre for low-resolution negative-ion MS measurements, and the MRC Biomedical NMR Centre for access to facilities.

REFERENCES

1. Wakelin, S., Conibear, P. B., Woolley, R. J., Floyd, D. N., Bagshaw, C. R., Kovacs, M., and Malnasi-Csizmadia, A. (2002) Engineering *Dictyostelium discoideum* myosin II for the introduction of site-specific fluorescence probes, *J. Muscle Res. Cell Motil. 23*, 673−683.
2. Yengo, C. M., Chrin, L. R., Rovner, A. S., and Berger, C. L. (2000) Tryptophan 512 is sensitive to conformational changes in the rigid relay loop of smooth muscle myosin during the MgATPase cycles, *J. Biol. Chem. 275*, 25481−25487.
3. Jameson, D. M., and Eccleston, J. F. (1997) Fluorescent nucleotide analogs: synthesis and applications, *Methods Enzymol. 278*, 363−390.
4. Cremo, C. R. (2003) Fluorescent nucleotides: Synthesis and characterization, *Methods Enzymol. 360*, 128−177.
5. Smith, C. A., and Rayment, I. (1996) Active site comparisons highlight structural similarities between myosin and other P-loop proteins, *Biophys. J. 70*, 1590−1602.
6. Bauer, C. B., Kuhlman, P. A., Bagshaw, C. R., and Rayment, I. (1997) X-ray crystal structure and solution fluorescence characterization of Mg•2′(3′)-*O*-(*N*-methylanthraniloyl)nucleotides bound to the *Dictyostelium discoideum* myosin motor domain, *J. Mol. Biol. 274*, 394−407.
7. Shutes, A., Phillips, R. A., Corrie, J. E. T., and Webb, M. R. (2002) The role of magnesium in nucleotide exchange on the small G protein rac, investigated using novel fluorescent guanine nucleotide analogues, *Biochemistry 41*, 3828−3835.
8. Webb, M. R., and Corrie, J. E. T. (2001) Fluorescent coumarin-labeled nucleotides to measure ADP release from actomyosin, *Biophys. J. 81*, 1562−1569.
9. Hutchinson, J. P., Rittinger, K., and Eccleston, J. F. (2000) Purification and characterization of guanine nucleotide dissociation stimulator protein, *Methods Enzymol. 325*, 71−82.
10. Rensland, H., Lautwein, A., Wittinghofer, A., and Goody, R. S. (1991) Is there a rate-limiting step before GTP-cleavage by H-ras p21? *Biochemistry 30*, 11181−11185.
11. Ma, Y., and Taylor, E. W. (1995) Kinetic mechanism of the kinesin motor domain, *Biochemistry 34*, 13233−13241.
12. Oiwa, K., Eccleston, J. F., Anson, M., Kikumoto, M., Davis, C. T., Reid, G. P., Ferenczi, M. A., Corrie, J. E. T., Yamada, A., Nakayama, H., and Trentham, D. R. (2000) Comparative single-molecule and ensemble myosin enzymology: sulfoindocyanine ATP and ADP derivatives, *Biophys. J. 78*, 3048−3071.
13. Brune, M., Hunter, J. L., Howell, S. A., Martin, S. R., Hazlett, T. L., Corrie, J. E. T., and Webb, M. R. (1998) Mechanism of inorganic phosphate interaction with phosphate binding protein from *Escherichia coli*, *Biochemistry 37*, 10370−10380.
14. Brune, M., Corrie, J. E. T., and Webb, M. R. (2001) A fluorescent sensor of the phosphorylation state of nucleoside diphosphate kinase and its use to monitor nucleoside diphosphate concentrations in real time, *Biochemistry 40*, 5087−5094.
15. Clark, R. J., Nyitrai, M., Webb, M. R., and Geeves, M. A. (2003) Probing nucleotide dissociation from myosin *in vitro* using μg quantities of myosin, *J. Muscle Res. Cell Motil. 24*, 315−321.

16. Khromov, A. S., Webb, M. R., Ferenczi, M. A., Trentham, D. R., Somlyo, A. P., and Somlyo, A. V. (2004) Myosin regulatory light chain phosphorylation and strain modulate adenosine diphosphate release from smooth muscle myosin, *Biophys. J. 86*, 2318−2328.
17. Weeds, A. G., and Taylor, R. S. (1975) Separation of subfragment-1 isoenzymes from rabbit skeletal muscle myosin, *Nature 257*, 54−56.
18. Lehrer, S. S., and Kerwar, G. (1972) Intrinsic fluorescence of actin, *Biochemistry 11*, 1211−1217.
19. Bershitsky, S., Tsaturyan, A., Bershitskaya, O., Mashanov, G., Brown, P., Webb, M. R., and Ferenczi, M. A. (1996) Mechanical and structural properties underlying contraction of skeletal muscle fibers after partial 1-ethyl-3-[3-(dimethylamino)propyl]carbodiimide cross-linking, *Biophys. J. 71*, 1462−1474.
20. Ozols, A. M., Azhavev, A. V., Dyatkina, N. B., and Krayevsky, A. A. (1980) Aminonucleosides and their derivatives. VI. A new synthesis of 1,2,5-tri-*O*-acyl-3-azido-3-deoxy-*β*-D-ribofuranose, *Synthesis*, 557−559.
21. Ghosh, A. K., and Liu, W. (1996) Total synthesis of (+)-sinefugin, *J. Org. Chem. 61*, 6175−6182.
22. Azhayev, A. V., Ozols, A. M., Bushnev, A. S., Dyatkina, N. B., Kochetkova, S. V., Victorova, L. S., Kukhanova, M. K., Krayevsky, A. A., and Gottikh, B. P. (1979) Aminonucleosides and their derivatives. IV. Synthesis of the 3′-amino-3′-deoxynucleoside 5′-phosphates, *Nucleic Acids Res. 6*, 625−643.
23. Cremo, C. R., Neuron, J. M., and Yount, R. G. (1990) Interaction of myosin subfragment 1 with fluorescent ribose-modified nucleotides. A comparison of vanadate trapping and SH1−SH2 cross-linking, *Biochemistry 29*, 3309−3319.
24. Hazlett, T. L., Moore, K. J. M., Lowe, P. N., Jameson, D. M., and Eccleston, J. F. (1993) Solution dynamics of p21ras proteins bound with fluorescent nucleotides: a time-resolved fluorescence study, *Biochemistry 32*, 13575−13583.
25. Corrie, J. E. T. (1994) Thiol-reactive fluorescent probes for protein labelling, *J. Chem. Soc., Perkin Trans. 1*, 2975−2982.
26. Corrie, J. E. T., Munasinghe, V. R. N., and Rettig, W. (2000) Synthesis and fluorescence properties of substituted 7-aminocoumarin-3-carboxylate derivatives, *J. Heterocycl. Chem. 37*, 1447−1455.
27. Fletcher, A. N., and Bliss, D. E. (1978) Laser dye stability. Part 5. Effect of chemical substituents of bicyclic dyes upon photodegradation parameters, *Appl. Phys. 16*, 289−295.
28. Leatherbarrow, R. J. (2001) *Grafit*, version 5, Erithacus Software Ltd., Horley, U.K.
29. McDevitt, J. P., and Lansbury, P. T. (1996) Glycosamino acids: new building blocks for combinatorial synthesis, *J. Am. Chem. Soc. 118*, 3818−3828.
30. Robins, M. J., Zou, R., Guo, Z., and Wnuk, S. F. (1996) Nucleic acid related compounds. 93. A solution for the historic problem of regioselective sugar-base coupling to produce 9-glycosylguanines or 7-glycosylguanines, *J. Org. Chem. 61*, 9207−9212.
31. Onodera, K., Hirano, S., and Masuda, F. (1967) Nucleosides and related substances. Part VI. The synthesis of 9-α-D-ribofuranosyladenine (α-adenosine), *Carbohydr. Res. 4*, 263−266.
32. Yoshikawa, M., Kato, T., and Takenishi, T. (1969) Studies of phosphorylation. III. Selective phosphorylation of unprotected nucleosides, *Bull. Chem. Soc. Jpn. 42*, 3505−3508.
33. Hoard, D. E., and Ott, D. G. (1965) Conversion of mono- and oligodeoxyribonucleotides to 5′-triphosphates, *J. Am. Chem. Soc. 87*, 1785−1788.
34. Hazlett, T. L., Jameson, D. M., Neal, S. E., Webb, M. R., and Eccleston, J. F. (1990) Time-resolved fluorescence studies of p21ras, *Biophys. J. 57*, 289a.
35. Siemankowski, R. F., Wiseman, M. O., and White, H. D. (1985) ADP dissociation from actomyosin subfragment 1 is sufficiently slow to limit the unloaded shortening velocity in vertebrate muscle, *Proc. Natl. Acad. Sci. U.S.A. 82*, 658−662.
36. Grabowski, Z. R., Rotkiewicz, K., and Rettig, W. (2003) Structural changes accompanying intramolecular electron transfer: focus on twisted intramolecular charge-transfer states and structures, *Chem. Rev. 103*, 3899−4031.
37. Chaurasia, C. S., and Kauffman, J. M. (1990) Synthesis and fluorescent properties of a new photostable thiol reagent "BACM", *J. Heterocycl. Chem. 27*, 727−733.
38. Hirshberg, M., Henrick, K., Haire, L. L., Vasisht, N., Brune, M., Corrie, J. E. T., and Webb, M. R. (1998) The crystal structure of phosphate binding protein labeled with a coumarin fluorophore, a probe for inorganic phosphate, *Biochemistry 37*, 10381−10385.

BI0486334